International Journal of Nanomedicine

Dovepress
open access to scientific and medical research

Open Access Full Text Article

ORIGINAL RESEARCH

# Bone Regeneration Revolution: Pulsed Electromagnetic Field Modulates Macrophage-Derived Exosomes to Attenuate Osteoclastogenesis

Martina Trentini[1,*], Ugo D'Amora[2,*], Alfredo Ronca[2], Luca Lovatti[2], José Luis Calvo-Guirado[3], Danilo Licastro[4], Simeone Dal Monego[4], Lucia Gemma Delogu[5], Mariusz R Wieckowski[6], Shlomo Barak[7], Oleg Dolkart[7], Barbara Zavan[1]

[1]Translational Medicine Department, University of Ferrara, Ferrara, 44121, Italy; [2]Institute of Polymers, Composites and Biomaterials - National Research Council (IPCB-CNR), Naples, 80125, Italy; [3]Faculty of Health Sciences, Universidad Autonoma de Chile, Santiago de Chile, 7500912, Chile; [4]AREA Science Park, Trieste, 34149, Italy; [5]Biomedical Science Department University of Padova, Padova, Italy; [6]Nencki Institute of Experimental Biology, Polish Academy of Sciences, Warsaw, Poland; [7]Magdent B.S.R. 3, Bnei Brak, Tel Aviv, Israel

*These authors contributed equally to this work

Correspondence: Alfredo Ronca; Barbara Zavan, Email alfredo.ronca@cnr.it; barbara.zavan@unife.it

**Introduction:** In the process of bone regeneration, a prominent role is played by macrophages involved in both the initial inflammation and the regeneration/vascularization phases, due to their M2 anti-inflammatory phenotype. Together with osteoclasts, they participate in the degradation of the bone matrix if the inflammatory process does not end. In this complex scenario, recently, much attention has been paid to extracellular communication mediated by nanometer-sized vesicles, with high information content, called exosomes (EVs). Considering these considerations, the purpose of the present work is to demonstrate how the presence of a pulsed electromagnetic field (PEMF) can positively affect communication through EVs.

**Methods:** To this aim, macrophages and osteoclasts were treated in vitro with PEMF and analyzed through molecular biology analysis and by electron microscopy. Moreover, EVs produced by macrophages were characterized and used to verify their activity onto osteoclasts.

**Results:** The results confirmed that PEMF not only reduces the inflammatory activity of macrophages and the degradative activity of osteoclasts but that the EVS produced by macrophages, obtained from PEMF treatment, positively affect osteoclasts by reducing their activity.

**Discussion:** The co-treatment of PEMF with M2 macrophage-derived EVs (M2-EVs) decreased osteoclastogenesis to a greater degree than separate treatments.

**Keywords:** PEMF, exosomes, macrophages, bone, osteoclast

## Introduction

As integral components of diverse cellular networks within the bloodstream, macrophages play a crucial role in orchestrating the intricate balance of bone homeostasis, repair, and growth. Their central involvement positions them as promising agents in advancing bone regeneration efforts. Upon implant insertion, macrophages swiftly migrate to the site of injury in response to chemical signals, influencing the fate of the implant.[1–4] These cells exhibit significant plasticity, capable of polarizing into either the pro-inflammatory M1 phenotype or the anti-inflammatory/healing M2 phenotype in response to the tissue microenvironment. M1 macrophages escalate inflammatory responses by generating large quantities of inflammatory cytokines (such as tumor necrosis factor-α [TNFα], IL-1, and IL-6) and reactive oxygen species (ROS). Conversely, M2 macrophages resolve inflammatory reactions and facilitate tissue repair through the secretion of anti-inflammatory and pro-regenerative factors (eg, IL-10 and transforming growth factor β [TGF-β]).[5–7] An imbalance in M1/M2 macrophage

Received: 9 May 2024
Accepted: 29 July 2024
Published: 24 August 2024

**Graphical Abstract**

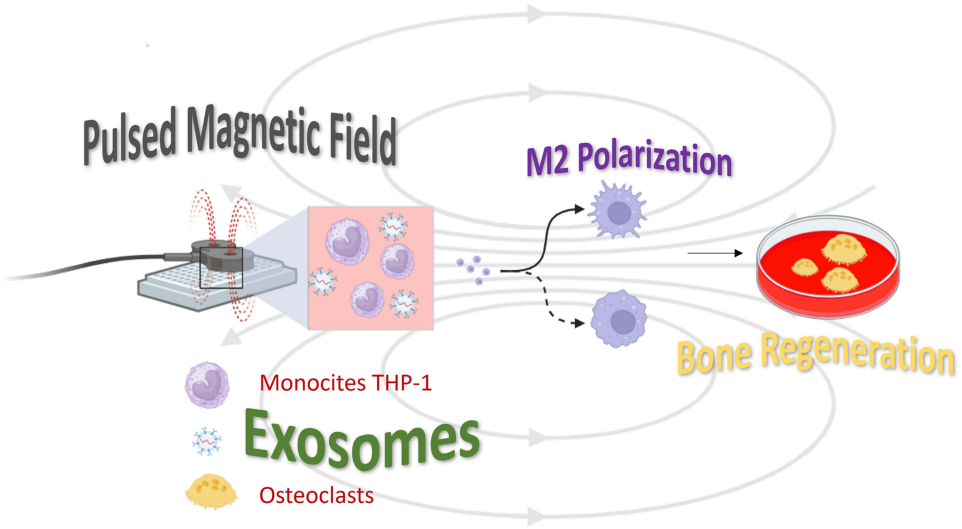


ratio, often due to prolonged presence of M1 macrophages, can lead to delayed tissue repair, the development of unresolved tissue damage and various inflammatory disorders. In recent years, considerable attention has been directed towards extracellular vesicles (EVs) as novel tools in regenerative medicine, with implications for wound healing, as well as regeneration of bone, cardiac tissue, and tendons, among other applications.[8–11] EVs are nanoscale vesicles released by various cells, with diameters typically ranging from 30 to 150 nm, and are found in various body fluids. Laden with biologically active substances such as proteins, lipids, DNA, and RNA, EVs play crucial roles in intercellular communication, signal transduction, and the regulation of biological processes including immune responses, cell proliferation, and differentiation.

It is widely acknowledged that EVs derived from mesenchymal stem cells (MSCs) play a crucial role in fostering bone regeneration by modulating osteogenic differentiation and gene expression via miRNA transfer. Moreover, MSC-derived EVs exhibit the capacity to enhance endothelial cell proliferation, migration, and tube formation by upregulating the vascular endothelial growth factor (VEGF) and hypoxia-inducible factor-1α (HIF-1α), thereby boosting the microvessel density in fractured bones. Certain genetic materials within these EVs can also induce M2 macrophage polarization by downregulating PRKCCD and PTEN expression, promoting p-AKT expression, and activating the PI3K/AKT signaling pathway.[12,13] Recent studies have shed light on the immunomodulatory properties of MSC-derived EVs, demonstrating their ability to promote the transition from M1 to M2 macrophage polarization and increase the secretion of anti-inflammatory cytokines and chemokines, offering therapeutic benefits in inflammatory conditions, wound healing, and tissue regeneration. Research by Yuki Nakao et al has revealed that EVs stimulated by TNF-α can facilitate M2 macrophage polarization by enhancing CD73 expression.[14,15] Similarly, Li et al have shown that EVs derived from adipose-derived stem cells (ADSCs) can effectively modulate the immune response surrounding bones, presenting a novel treatment approach to enhance bone healing. Recent findings suggest that macrophages may employ a paracrine mechanism to create an optimal microenvironment for reducing inflammation, with EVs playing a crucial role in mediating interactions with neighboring cells and influencing cytokine and miRNA levels to attenuate inflammatory responses in recipient cells. In a mouse model of inflammatory pain, EVs derived from macrophages have been observed to mitigate thermal hyperalgesia, highlighting their involvement in regulating dysregulated inflammation. However, the extent to which polarized macrophages contribute to osteoclast differentiation through EV secretion remains incompletely understood.[16–20]

Alongside this novel nano biobased technology, recent studies have shown that also physical treatments, such as PEMF, can be used as innovative therapy for inflammatory management, with potentially substantial benefits in regenerative therapies.[21,22] Evidences showed that PEMF treatment increased bone formation, and was able to decrease bone resorption in the monoiodoacetic acid-induced (MIA) osteoarthritis (OA) rat model.[23] Moreover, it has been demonstrated that PEMF is able to modulate both cell surface receptor expression/activation and downstream signal transduction pathways, restoring homeostatic cell functions such as viability, proliferation, differentiation, communication with neighboring cells, and interaction with extracellular matrix (ECM) components.[24,25] Indeed, the continuous and prolonged exposure of cells to magnetic fields modifies cell physiological activities such as proliferation, accelerates cell differentiation, increases the deposition of collagen and the synthesis and secretion of growth factors, and modulates the activation of cell surface receptors, thereby holding relevant contributions for the re-establishment of homeostatic cell functions.[23,26–29] PEMF exposure has also been shown to exert anti-inflammatory effects by up-regulating A2A and A3 adenosine receptors (ARs), thereby mitigating the expression of pro-inflammatory cytokines.[30] Some studies have also underlined how extremely low-frequency PEMF may provide advantages for in vitro tissue generation, stimulating angiogenesis and promoting bone formation, and modulating inflammatory response in MSCs and macrophages.[26,31–33]

Therefore, PEMF stimulation may play a crucial role in the inflammatory process of injured tissues, resulting in enhanced functional recovery and support tissue regeneration both in a direct or indirect way.[34–38]

Synergistically combining EVs with PEMF could be a promising strategy in which EVs not only play an osteogenic role but also inhibit the excessive inflammatory response, and promote bone healing. However, the effect of PEMF on EVs in promoting bone regeneration and inhibiting inflammatory response has not still in depth investigated. This study aimed at exploring the regulatory effect of PEMF on bone regeneration and inflammatory response of macrophage derived EVs through in vitro experiments. The finding will open a new direction for enhancing the therapeutic effect of PEMF, demonstrating that it not only reduce the inflammatory activity of macrophages and the degradative activity of osteoclasts but that macrophage derived EVs significantly attenuate the secretion of pro-inflammatory cytokines and positively affect osteoclasts by reducing their activity. Furthermore, given their heightened anti-inflammatory potential, EVs will be a promising approach for accelerating bone formation and reducing inflammation in the bone regeneration process.

# Materials and Methods

## Cell Culture and PEMF Exposure

The THP-1 monocyte cell line, acquired from Resnova (Rome, Italy), underwent culture at Roswell Park Memorial Institute (RPMI) 1640 complete medium (Euroclone S.P.A, Pero, Italy) and 10% Fetal bovine serum (FBS, Euroclone S. P.A., Pero. Italy). Cultures were maintained at 37°C with 5% $CO_2$, and the medium was refreshed every 2 days. For experimental purposes, differentiation of THP-1 monocytes into macrophages was achieved by exposure to a complete RPMI 1640 medium containing 100 ng/mL of Phorbol 12-myristate 13-acetate (PMA) for 24 hours, followed by a 72-hour resting period. During this interval, adhered macrophages were cultured in complete RPMI 1640 medium.

RAW264.7 cells were procured from Sigma-Aldrich, Milan, Italy. To study osteoclastogenesis, α minimum essential media (α MEM; Gibco; Thermo Fisher Scientific, Inc., Waltham, MA, USA) supplemented with 10% FBS and 1% penicillin/1% streptomycin, along with 50 ng/mL RANK-L (PeproTech, Inc., Rocky Hill, NJ, USA) was utilized to culture these cells. For the application of PEMF, the cells were housed in an incubator containing the Magdent's electromagnetic healing abutments (Magdent ltd-Kinneret St 5, Bnei Brak, Israel) present in the bottom of the petri dishes. Cells in the control group were housed in a separate incubator under identical conditions but without PEMF exposure. The devices used in this study were miniaturized PEMF devices designed to resemble healing abutments (healing caps) for dental implants, featuring a 1.25 mm (0.05") hexagonal socket. Constructed with a Ti6Al4V (Grade 5) structure, each PEMF device comprised a battery serving as a power source, an electronic component, and a coil. Upon activation, the device emitted an electromagnetic field with a radius of 2 mm, an exposure ratio ranging from 1/500 to 1/5000, intensity levels spanning from 0.05 to 0.5 mT, and a frequency between 10 and 50 kHz. Activation of the device

was facilitated by insertion into an activator apparatus employing a magnetic mechanism to initiate the battery. Subsequently, the PEMF emitted the electromagnetic field continuously for a duration of 30 consecutive days.

## Scanning Electron Microscopy

A morphological assessment of cultured cells was conducted using 2D scanning electron microscopy (SEM Zeiss EVO 40, Zeiss, Oberkochen, Germany). In this study, $3\times10^5$ THP-1 cells were seeded onto sterile coverslips coated with poly-d-lysine and induced to differentiate into macrophages. Following the treatment, all samples were fixed with 2% glutaraldehyde in phosphate buffer (PBS, Sigma-Aldrich, Milan, Italy) at 4°C, dehydrated using a series of ethanol baths with increasing concentrations, mounted, and then sputter-coated with gold following standard procedures. Imaging was performed under high vacuum conditions using a secondary electron detector.

## EVs Isolation and Analyses

EVs were isolated from the conditioned medium (CM) of cells using the Cell Culture Media EV Purification Kit (Norgen Biotek Corp., ON, Canada) in accordance with the manufacturer's instructions. For transmission electron microscopy (TEM) analysis using the TEM Zeiss EM 910 instrument (Zeiss, Oberkochen, Germany), EVs were fixed in a 2% glutaraldehyde solution in PBS at a ratio of 1:1. Subsequently, the EVs were deposited, rinsed, and stained with heavy metal compounds onto a gridded slide following standard protocols. The distribution size and diameter of EVs were assessed using the qNano platform (iZON Science, UK). The analyses were conducted employing NP150 nanopores and CPC200 calibration particles under a pressure of 20 mbar. The obtained results were analyzed with the Izon control suite v3.4. The Elisa analysis of EVs specific markers was performed using the commercial Exo-Check™ exosome antibody array (Systems Biosciences, USA), according to the manufacturer's instructions. The array contains eight known EVs markers, including CD63, CD81, ALIX, FLOT1, ICAM1, EpCam, ANXA5, and TSG101; four controls, including two positive controls (HRP Detection), blank spot (background control) and GM130 cis-Golgi marker, which monitors for any cellular contamination. Briefly, 50 µg of MSC-EVs was lysed and labeled for 30 min with constant mixing. The labeled samples were washed and blocked with a blocking buffer. Array membrane was incubated with labeled lysate/blocking buffer mixture at 4°C overnight on a rocker. The next day, the samples were washed and incubated with a detection buffer for 30 min at RT on a shaker and analysed by the chemiluminescence imaging system (ChemiDoc, Bio-Rad). Experiments were performed in triplicate.[9,29,38–40]

## Sequencing and Data Analysis

NanoDrop 2000 (Thermo Fisher Scientific, Waltham, MA, USA) and Agilent Bioanalyzer 2100 (Agilent, Santa Clara, CA, USA) were employed to assess total RNA. Libraries were created with 1 µg of total RNA by TruSeq Sample Preparation RNA Kit (Illumina Inc., San Diego, CA, USA) according to the manufacturer's protocol. All libraries were quantified with Qubit dsDNA BR Assay Kit (Thermo Fisher Scientific, Waltham, MA, USA) on Qubit 2.0 Fluorometer (Thermo Fisher Scientific, Waltham, MA, USA). RNA sequencing was realized on Novaseq 6000 sequencer (Illumina Inc., San Diego, CA, USA) according to the manufacturer's protocol. FASTQ files as output were performed with Illumina BCLFASTQ v2.20 software. All raw files quality was verified with FASTQC software and low-quality sequence was discarded from the analysis. Specified reads were aligned to the complete human genome using Splices Transcripts Alignment to a Reference algorithm STAR version 2.7.3 with hg38 Genome Assembly and Genecode.v35 as gene definition. Resulting mapped reads were included as input for feature count functions of Rsubread packages and were used as gene counts for differential expression analysis using Deseq2 package. Reads comparison was performed between EVs-treated THP-1-derived macrophages and osteoclasts and untreated THP-1-derived macrophages and osteoclasts. Differentially expressed genes (DEGs) were selected for log 2 (FR) $< -1$ or $> 1$ and p-value $< 0.05$.

MiRNA-Seq libraries were prepared using the QIAseq miRNA Library Kit (QIAGEN; Hilden, GE) and sequenced using Novaseq 6000 (Illumina; San Diego, CA, USA) in 2×150 paired-end mode. In the samples, miRNAs were identified by means of the QIAseq miRNA-NGS data analysis software considering Single Read as read type and Read 1 Cycles 75 as read cycles.

All datasets from RNA sequencing and miRNA sequencing were analyzed with the Qiagen Ingenuity Pathway Analysis (IPA) software. For RNA sequencing analysis, IPA categorized all DEGs in canonical pathways. IPA can make a prediction on possible disease and functions, which were ranked based on their significance (p-value) and predicted state of activation/inhibition (z-Score). Z-Score value has been set with cut-off < −2 or > +2. RNA sequencing was used to perform functional, biological pathway, biological process and cellular component enrichment with FunRich software.[37] Functional enrichment for miRNA sequencing was performed with miRNet on Reactome Biological Pathway database. Furthermore, it provides miRNA target gene data that were collected from four well-annotated database miRTareBase v8.0. All miRNet enrichment was reported with Prism 8.03 software graphical view (GraphPad Software Inc, Boston, MA, USA).

## Fluorescence Labelling and Imaging

EVs were stained with PKH26 membrane labelling fluorophore (Sigma-Aldrich, St. Louis, MO, USA). According to an adapted manufacture's protocol, 0.8 µL PKH26 in 200 µL Diluent C was added to PBS, resuspended in Diluent C after isolation, to 400 µL as final volume. After that, the mix was first incubated for 5 min at room temperature to allow staining; after, it was subsequentially moved to 30 K membrane centrifugal filters (Amicon Ultra-0.5, Millipore, Burlington, MA, USA) and centrifugated at 14,000× *g* for 20 min to remove the dye excess. Stained EV and PBS were used for cell-line treatment as described above. At the end of the experimental treatment, the cells were fixed with 4% PFA and stained with phalloidin Alexa Fluor 488. Imaging was performed with a confocal microscope Nikon ECLIPSE Ti equipped with DS-Qi2 camera, 40× air and 60× immersion objectives.

## RNA Extraction, Sequencing, and RT-qPCR

The extraction of total RNA from THP-1-derived macrophages and osteoclasts post-treatment with EVs at a concentration of $10^6$/mL was carried out using the Total RNA Purification Plus Kit (Norgen Biotek Corp., Thorold, ON, Canada), following the manufacturer's instructions tailored for cells cultured in a monolayer. Subsequently, the quality and concentration of the extracted RNA were assessed using the NanoDrop One (Thermo Fisher Scientific, Waltham, MA, USA), after which the RNA samples were stored at −80°C until further analysis. To generate first-strand cDNA from the total RNA, 1200 ng of RNA from each sample was reverse transcribed using the SensiFAST cDNA Synthesis Kit (Meridian Bioscience, Cincinnati, OH, USA) in a final volume of 20 µL. Real-time quantitative PCR (qPCR) was then performed using primers listed in Table 1, employing the GDS Rotor-Gene® Q Thermocycler (QIAGEN, Hilden, Germany) with SensiFAST SYBR No-ROX master mix (Meridian Bioscience, Cincinnati, OH, USA) following the manufacturer's protocol. The qPCR cycling conditions included an initial PCR activation step at 95°C for 2 min, followed by 40 cycles comprising denaturation at 95°C for 5 s, annealing at 60°C for 10s, and extension at 70°C for 20s. Finally, the melting temperature of the amplicons was analyzed by gradually increasing the temperature from 72°C to 95°C over a span of 5 min.

## Statistical Analysis

For Ingenuity Pathway Analysis (IPA), data are presented as means ± standard error of the mean (SEM). Single comparisons were assessed using the Student's *t*-test, while a one-way analysis of variance (ANOVA) was utilized for multiple comparisons. A significance level of $p < 0.05$ was employed to determine the statistical significance.

**Table 1** Primer Sequences for RT-PCR

| Gene | Frw | Rev | Length |
|---|---|---|---|
| Tyrosine-protein kinase (CSK) | TCGGGTGGAGAAGGGCTACAA | CAGGTGCAGCTCGTGGGTTT | 160 |
| Nuclear Factor of Activated T Cells 1 (NFATC1) | CGGGAAGAAGATGGTGCT | CTGGTTGCGGAAAGGTGGTA | 169 |
| Tartrate-resistant acid phosphatase (TRAP) | CAATGCCAGCGTCCCTTCCAAA | TTCTTCCTCCCGATGTCCGTCT | 167 |
| MicroRNA 7–1 (miR-7) | UGGAAGACUAGUGAUUUUGUUGUU | CAACAAAUCACAGUCUGCCAUA | 164 |
| MicroRNA 1897 (miR-1897) | TCTTCA AGTCCG CCATGCCCG | CTACCCCGACCACATGAAGC | 163 |

In all other analyses, results are reported as mean ± standard deviation (SD), along with the standard error (SE) derived from at least three independent replications of the experiment. Group differences were evaluated using analysis of variance (ANOVA), with post hoc Bonferroni testing for multiple comparisons. Statistical significance is indicated as follows: *$p < 0.05$, °$p < 0.01$, §$p < 0.001$, and #$p < 0.0001$.

# Results

## PEMF Action on Osteoclast Activity

RAW264.7 cells were cultured in the presence of RANK-L to evaluate osteoclastogenesis activity. To this aim, expression analysis of specific genes such as CTSK, NFATC1, TRAP, miR-7 and miR-1897 was performed. As reported in Figure 1, in the case of RANK-L treatment (orange bars), all these genes resulted up-regulated compared to the control (no RANK-L treatment, blue bars). The combined treatment by PEMF and RANK-L (grey bars) induced a well-defined decrease in osteoclastic activity for all selected genes, meanwhile the only presence of PEMF (yellow bars) did not affect osteoclasteogenetic activity of the cells.

## PEMF Action on Macrophages Commitment

THP-1 cultures in the presence or absence of PEMF were analysed in terms of morphological features by SEM analysis. As reported in Figure 2A and B), in the absence of PEMF, THP-1 treated with inflammatory stimulus, acquired a M1 inflammatory-like morphology, as highlighted by a big round shape. In contrast to PEMF treatment, even in the presence of inflammatory stimuli, cells acquired a fusiform shape, associated to a M2 anti-inflammatory-like morphology (Figure 2C and D).

Total RNA extracted from macrophages cultured in the presence of PEMF action was sequenced, and ingenuity pathway analysis (IPA) was carried out on differentially expressed genes (DEGs). Thirty-four genes were significantly de-regulated in macrophages treated with PEMF (Figure 3). Among these, 5 genes related to M1 commitment such as IRAK3, IRF8, DNMT1, TNFAIP2 and IL6R were down-regulated; and 8, related to M2 commitment such as EGR2, IL4R, STAT6, IL4I1, PPARD, MRC1, IL10RA, FN1 were up-regulated.

IPA canonical pathways revealed that these genes were associated to biological pathways related to the immune system (Figure 4A and B). In detail the main involved pathways were related to IL6 and 1 and they were down-regulated, confirming the anti-inflammatory activity of PEMF, and increasing on TCTP pathway related to the M2 commitment.

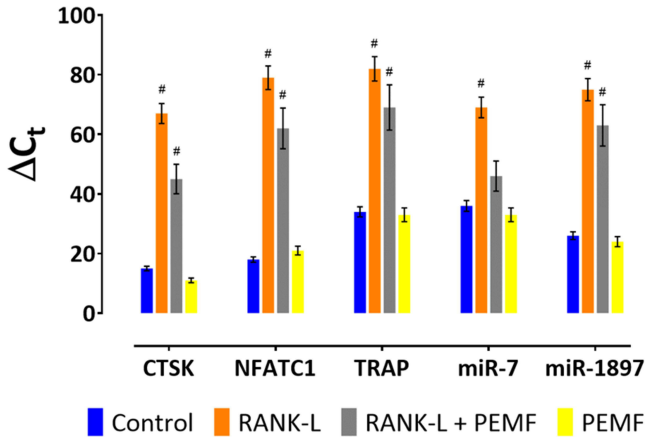


**Figure 1** Gene expression related to osteoclastogenesis activity of RAW264.7: CTSK, NFATC1, TRAP; miR-7, miR-1897. Orange bars are related to RANK-L treatment. Blue bars are related to the control (no RANK-L treatment). Grey bars are related to the presence of PEMF and RANK-L, yellow bars are related to PEMF. Statistical analysis of variance of the means between each group and the respective control was assessed by ANOVA and post hoc Bonferroni testing [#$p < 0.0001$].

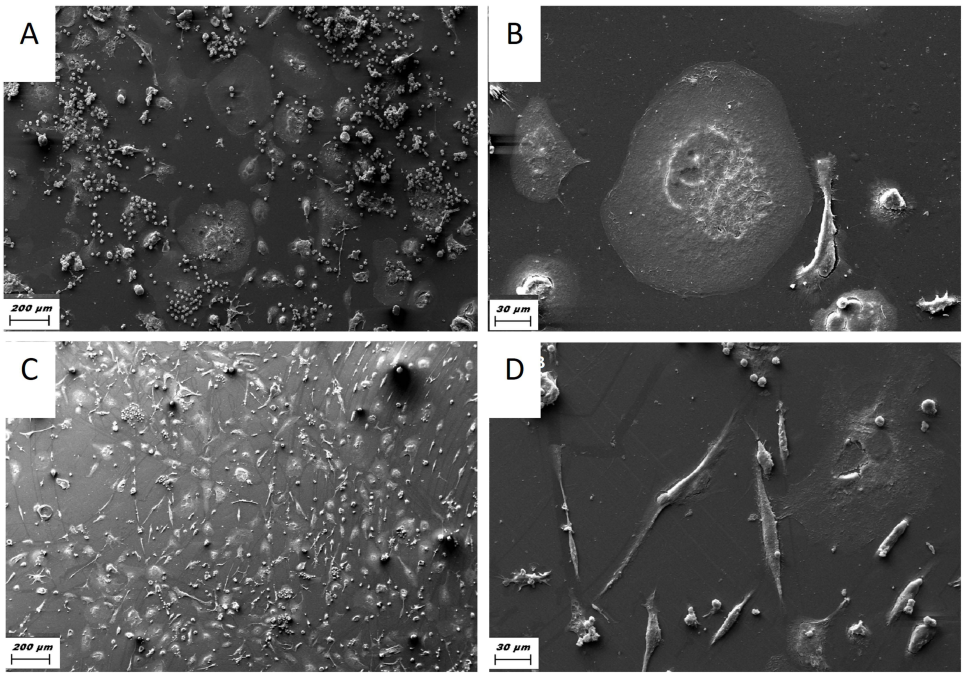


**Figure 2** SEM analyses of THP-1: (**A** and **B**) in normal conditions, cells acquire a round morphology typical of M1 phenotype; meanwhile, (**C** and **D**) in presence of PEMF, they acquire a fusiform morphology typical of M2 phenotype. (**A** and **C**) Scale Bar: 200 µm, (**B** and **D**) Scale Bar: 30 µm.

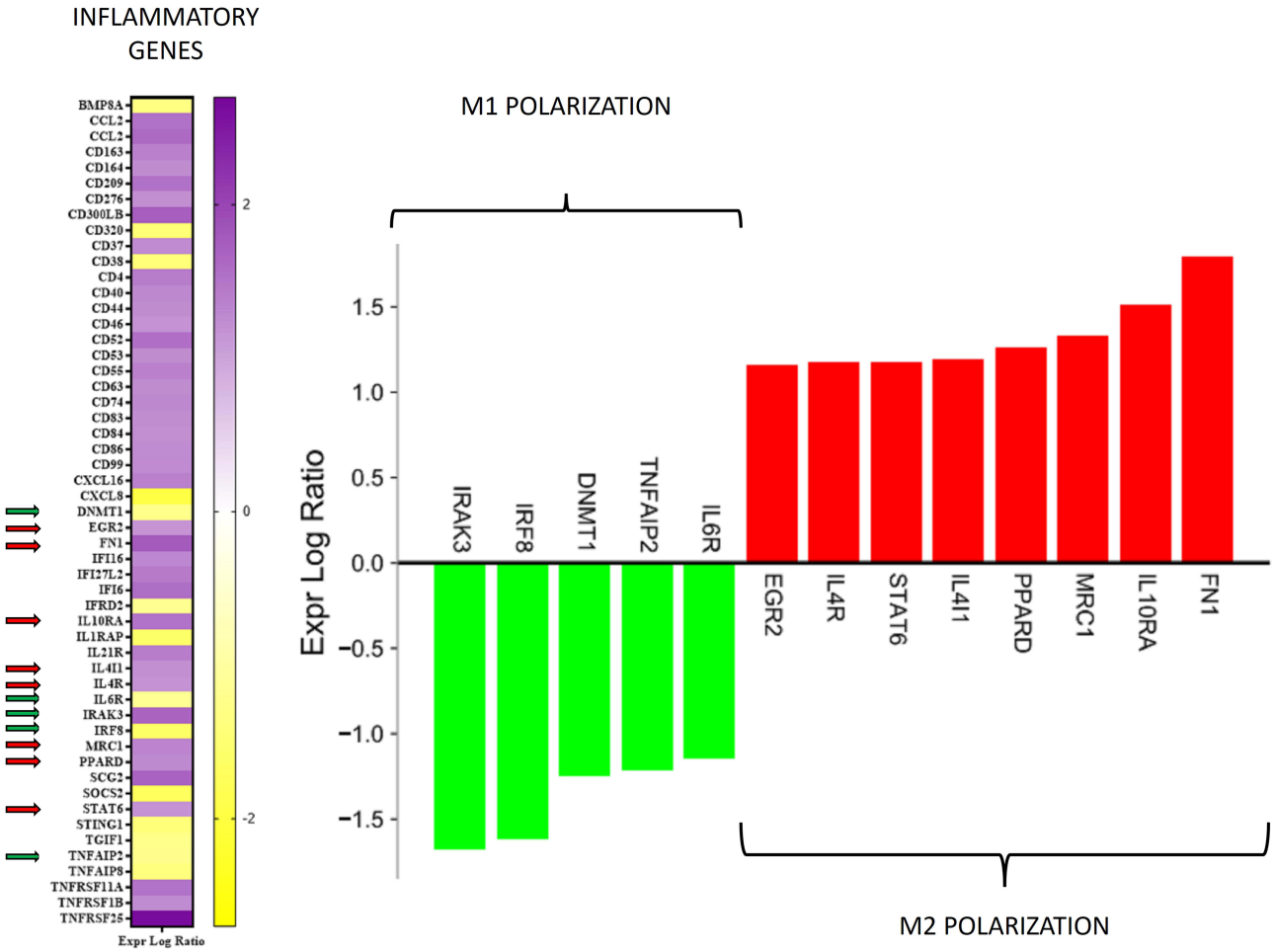


**Figure 3** Heat map and histogram related to gene expression of principal genes expressed by THP-1 cells in presence of PEMF.

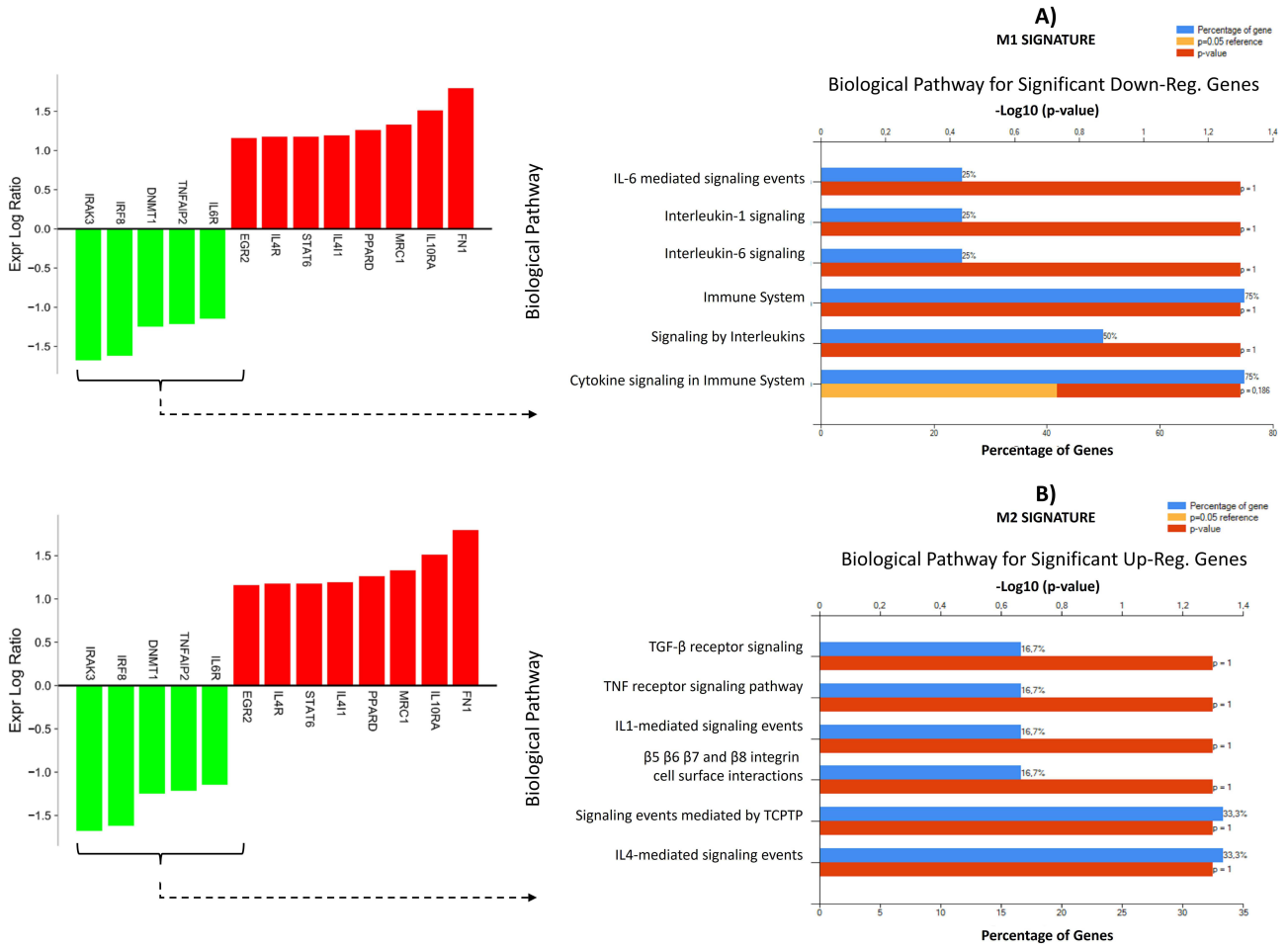


**Figure 4** IPA canonical pathways of (**A**) down-regulated genes, and (**B**) up-regulated genes.

## EVs from Macrophages M2 Reduce Osteoclastogenesis

M2-derived EVs (M2-EVs) were isolated and analysed with qNano to define their size and distribution. As reported in Figure 5, the analysis confirmed that M2 was able to produce EVs with a size ranging from 110 to 150 nm (Figure 5A). The TEM confirmed the same size (Figure 5B); meanwhile, the correct protein content, direct to identified EVs such as CD63, CD81 CD90 is reported in Figure 5C. When osteoclasts were incubated with M2-derived EVs, they were recognized and internalized as clearly reported in Figure 5D, where osteoclasts show red nano spot (the EVs) in intracellular space.

The effect of these EVs on osteoclasts was assessed by means of gene expression of the principal osteoclastogenetic related genes such as CTSK, NFATC1, TRAP, miR-7, miR-1897. As reported in Figure 6, treatment of RANK-L induced an increase of the genes, confirming the correct commitment process, the presence of EVs induced a reduction on this process (green bars) that was maximized when M2-EVs type were in presence of PEMF (red bars).

# Discussion

Treating bone disorders clinically still presents challenges, particularly in managing bone resorption mediated by osteoclasts. The efficacy of modern implantology hinges on the quality of new bone formation around implants.[41–44] Bone regeneration follows a sequential process comprising inflammation, proliferation, and remodeling phases. Each phase is integral, as proper progression is essential for tissue regeneration. The inflammation phase is pivotal as it primes the extracellular environment for subsequent proliferation and differentiation. However, prolonged inflammation can lead to peri-implantitis, a known complication characterized by bone loss around the implant, ultimately resulting in implant

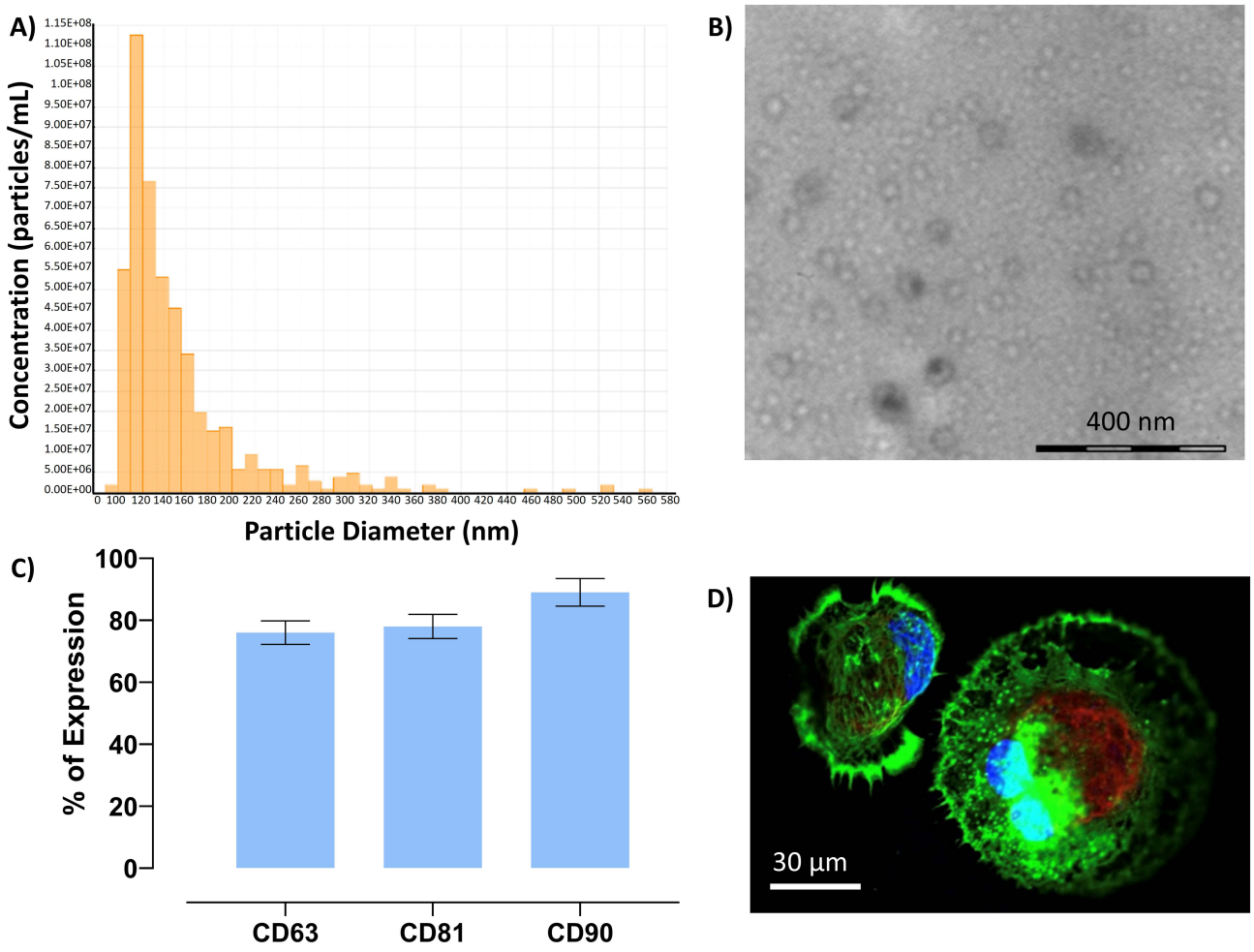


**Figure 5** Analyses of EVs: (**A**) Particle size distribution and concentration of EVs analyzed by tunable resistive pulse sensing: mean diameter of 100 ± 20.9 nm, mode of 65 nm. (**B**) Representative image of EVs at TEM. EVs appear with the typical bilayer cup-shaped membrane structure. (**C**) Elisa for EVs showing positivity to surface markers: CD63 CD81 and CD90. (**D**) Representative image of the uptake of PKH26-labeled red fluorescent EVs from macrophage after 24 h of incubation. Nuclei stained with Hoechst 33342 (blue).

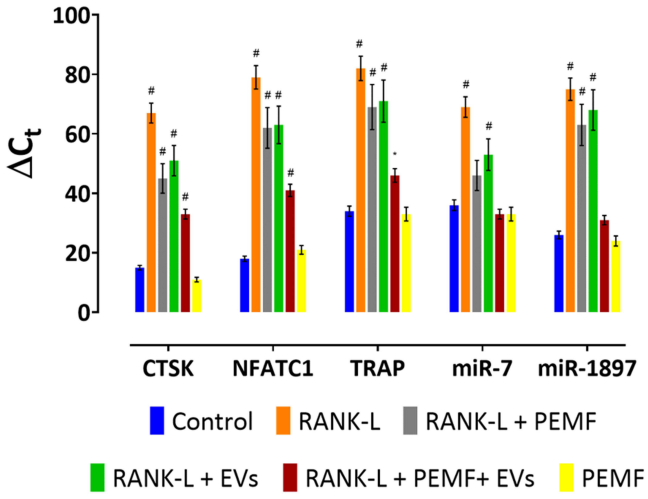


**Figure 6** Gene expression related to osteoclastogenesis activity of RAW264.7: CTSK, NFATC1, TRAP; miR-7, miR-1897. Orange bars are related to RANK-L treatment. Blue bars are related to the control (no RANK-L treatment). Grey bars are related to the presence of PEMF and RANK-L, green bars are related to RANK-L plus EVs, red bars are related to RANK-L plus PEMF plus EVs, yellow bars are related to PEMF alone. Statistical analysis of variance of the means between each group and the respective control was assessed by ANOVA and post hoc Bonferroni testing [*$p < 0.05$; #$p < 0.0001$].

failure. The primary drivers of bone resorption are osteoclasts, which degrade the bone matrix. In this study, we utilized an osteoclast cell line capable of activation in the presence of RANK-L. We investigated how genes associated with bone degradation are affected by PEMF. Figure 1 illustrates that the absence of RANK-L does not trigger the expression of osteoclast activation-related genes, even in the presence of PEMF. Conversely, the presence of RANK-L significantly upregulates osteoclast genes such as CTSK, NFATC1, miR-7, and miR-1897 in agreement with the results of Zhang et al.[45] However, even if previous research has shown that PEMF can influence biological processes by altering electromagnetic fields as showed by Chen et al,[46] in this study, PEMF stimulation was employed to modulate macrophage-derived EVs. Notably, a reduction in the expression of these genes was observed when activator or RANK-L treatment was combined with PEMF treatment, suggesting that PEMF reduces osteoclast lytic activity.

Another critical aspect contributing to bone loss is the chronic inflammatory environment around implants. Macrophages, particularly in the M1 inflammatory state, play a central role in this process by generating inflammatory cytokines and metalloproteinases that degrade the ECM, alongside osteoclasts that degrade the mineralized matrix. Thus, finding new strategies to address these challenges is imperative. Macrophages can transition from the pro-inflammatory M1 phenotype to the anti-inflammatory M2 phenotype, facilitating tissue regeneration. Failure of macrophages to transition to the M2 state impedes the regeneration phase. Anticipating and promoting this transition is therefore crucial for accelerating healing. Our findings, both morphologically and molecularly, confirm that PEMF expedites the formation of macrophages into the M2 phenotype.

Indeed, monocytes, when placed in culture in the presence of inflammatory factors, spontaneously acquire an M1 phenotype, as well documented by the SEM images in Figure 2. Conversely, if the same treatment was performed in the presence of PEMF, the phenotype acquired by the monoliths (THP-1) was M2 type.

This transition was validated and documented by the molecular biology (RNA sec) analyses, shown in Figure 3. As it is evident, the presence of PEMF reduced the expression of markers related to the M1 phenotype such as: IRAK3, IRF8, DNMT1, TNFAIP2, IL6R. This gene induced a down regulation of the following pathways: interleukin mediated signaling event, immune system, cytokine signaling as reported in Figure 4A. By contrast, there was a clear increase in genes related to the M2 anti-inflammatory phenotype, such as EGR2, IL4R, STAT6, FN1, IL4I1, IL10RA, PPARD, MRC1 involved in the up-regulation of the following pathways: TGF-β receptor signaling, TNF receptor signaling pathway, IL1-mediated signaling event, β7 and β8 integrin cell surface interaction, signaling events mediated by TCPTP, IL4-mediated signaling event (Figures 3 and 4B).

Analyzing all these data led to the conclusion that the main activities exerted by PEMF of macrophages can be summarized in reduction on chemotaxis of leukocytes, killing of bacteria, inflammatory response, increasing of vasculogenesis and survival of organism.

Finally, it was analyzed whether PEMF could affect the ability of positive communication between cells and thus indirectly influence tissue regeneration. To this end, M2-EVs phenotype and treated activated osteoclasts were investigated. As it is well known, EVs are vesicles with high information content capable of transporting information from one cell to another. Previous studies, by Song et al and Zhou et al, have demonstrated that M2-EVs decrease osteoblast development of bone marrow mesenchymal stem cells and Periodontal Ligament Stem Cells (PDLSCs) and boost pro-inflammatory cytokines.[47,48] Moreover, Chen et al demonstrated that the reparative M2-like macrophages could promote osteogenesis while inhibiting osteoclastogenesis in vitro and in murine periodontitis models via IL-10 mRNA. Nevertheless, it is not deeply studied how M2-EVs affects mononuclear macrophage osteoclastogenesis.[49] In this work the process of EV isolation was followed by the distribution, morphological and receptor analysis and the images confirmed that the isolated vesicles were indeed EVs and that activated macrophages were able to endocytose them.

Activated osteoclasts were then treated with both M2 macrophage derived EVs and PEMF and analyzed for expression of markers related to the process of bone lysis. As shown in Figure 6, the presence of these EVs amplified the beneficial effect of PEMF by dramatically reducing the expression of lytic genes confirming also the results of the work from Zhou et al.[48,50–53]

## Conclusions

In the present study, the combined effect of PEMF and EVs on bone regeneration was investigated. The overall results confirmed that magnetic fields may positively influence bone regeneration, acting on both osteoclastogenesis and inflammation. Regarding osteoclastogenesis, PEMF was able to reduce the osteoclastogenesis of THP-1 monocytes, after activation with RANK-L. Furthermore, they induced a secretion of EVs from macrophage M2 able to reduce osteoclastogenesis. Regarding inflammation, PEMF induced the commitment of macrophages from M1 phenotype to M2. Considering these observations, the present work sheds light on the transformative potential of PEMF and EVs-mediated communication within the context of bone remodeling. Our findings unveil novel mechanisms through which PEMF and EVs orchestrate the intricate process of bone resorption, offering valuable insights into their synergistic interplay and potential therapeutic implications. Our study suggests that EVs, which are nanoscale vesicles secreted by macrophages in response to PEMF stimulation, play a pivotal role as mediators of intercellular communication in bone regeneration. These EVs are rich in a diverse array of bioactive molecules, including proteins, lipids, and nucleic acids. Importantly, our data demonstrate that these EVs act as potent regulators of osteoclast activity, exerting inhibitory effects on bone resorption and creating an environment conducive to tissue repair. This finding underscores the crucial role of EVs-mediated signaling in modulating osteoclastogenesis and highlights the potential for EVs to influence bone remodeling by maintaining a delicate balance between bone formation and resorption. However, it is important to note that while our study provides compelling evidence for the inhibitory effects of EVs on osteoclast activity, it does not extend to their impact on osteos and overall bone formation. Therefore, the assertion that EVs promote bone regeneration must be tempered by acknowledging this limitation. Comprehensive molecular analyses of EVs cargo, including miRNAs and growth factors, were not conducted in this study. Future research should aim to characterize these components to fully elucidate their role in bone remodeling processes. Moreover, while our in vitro findings are promising, in vivo studies are essential to validate the observed effects of PEMF and EVs on bone regeneration. Such studies would provide a more holistic understanding of the therapeutic potential of PEMF and EVs-mediated communication in clinical settings. In conclusion, this study represents a significant step towards understanding how PEMF and EV-mediated communication could be harnessed for therapeutic purposes. By identifying the intricate interplay between inflammation, cellular communication, and tissue regeneration, our findings pave the way for innovative therapeutic strategies aimed at enhancing bone repair and mitigating implant-related complications. Despite the limitations of our study, including the need for in vivo validation and comprehensive molecular analysis of EVs cargo, the insights gained here lay the groundwork for future research aimed at developing targeted therapies that leverage the synergistic potential of PEMF and EVs in bone regeneration.

## Data Sharing Statement

The data will be available from the corresponding authors.

## Acknowledgments

Centro di Microscopia Elettronica of Ferrara University (Ferrara, Italy) is kindly acknowledged for performing SEM analysis, while by Area Science Park (ASP, Trieste, Italy) is acknowledged for mRNA sequencing and miRNA profiling with Illumina sequencing.

## Author Contributions

All authors made a significant contribution to the work reported, whether that is in the conception, study design, execution, acquisition of data, analysis and interpretation, or in all these areas; took part in drafting, revising or critically reviewing the article; gave final approval of the version to be published; have agreed on the journal to which the article has been submitted; and agree to be accountable for all aspects of the work.

## Funding

This project was supported by University of Ferrara, grant number 2022BZ.

## Disclosure

Professor Shlomo Barak is the chairman of the board of Magdent Ltd. Dr Oleg Dolkart is a consultant for Magdent Ltd. The authors report no other conflicts of interest in this work.

## References


1. Michalski MN, McCauley LK. Macrophages and skeletal health. *Pharmacol Ther*. 2017;174:43–54. doi:10.1016/j.pharmthera.2017.02.017
2. Alvarez MM, Liu JC, Trujillo-de santiago G, et al. Delivery strategies to control inflammatory response: modulating M1-M2 polarization in tissue engineering applications. *J Control Release*. 2016;240:349–363. doi:10.1016/j.jconrel.2016.01.026
3. Bai L, Du Z, Du J, et al. A multifaceted coating on titanium dictates osteoimmunomodulation and osteo/angio-genesis towards ameliorative osseointegration. *Biomaterials*. 2018;162:154–169. doi:10.1016/j.biomaterials.2018.02.010
4. Zhao S, Mi Y, Guan B, et al. Tumor-derived exosomal miR-934 induces macrophage M2 polarization to promote liver metastasis of colorectal cancer. *J Hematol Oncol*. 2020;13(1):156. doi:10.1186/s13045-020-00991-2
5. Guihard P, Danger Y, Brounais B, et al. Induction of osteogenesis in mesenchymal stem cells by activated monocytes/macrophages depends on oncostatin m signaling. *Stem Cells*. 2012;30(4):762–772. doi:10.1002/stem.1040
6. Ma Q, Liao J, Cai X. Different sources of stem cells and their application in cartilage tissue engineering. *Curr Stem Cell Res Ther*. 2018;13 (7):568–575. doi:10.2174/1574888X13666180122151909
7. Jin SS, He DQ, Luo D, et al. A biomimetic hierarchical nanointerface orchestrates macrophage polarization and mesenchymal stem cell recruitment to promote endogenous bone regeneration. *ACS Nano*. 2019;13(6):6581–6595. doi:10.1021/acsnano.9b00489
8. Mahon OR, Browe DC, Gonzalez-Fernandez T, et al. Nano-particle mediated M2 macrophage polarization enhances bone formation and MSC osteogenesis in an IL-10 dependent manner. *Biomaterials*. 2020;239:119833. doi:10.1016/j.biomaterials.2020.119833
9. Ferroni L, Gardin C, D'Amora U, et al. Exosomes of mesenchymal stem cells delivered from methacrylated hyaluronic acid patch improve the regenerative properties of endothelial and dermal cells. *Biomater Adv*. 2022;139:213000.
10. Liu X, Li Q, Niu X, et al. Exosomes Secreted from Human-Induced pluripotent stem cell-derived mesenchymal stem cells prevent osteonecrosis of the femoral head by promoting angiogenesis. *Int J Biol Sci*. 2017;13(2):232–244. doi:10.7150/ijbs.16951
11. Zhang Y, Bi J, Huang J, Tang Y, Du S, Li P. Exosome: a review of its classification, isolation techniques, storage, diagnostic and targeted therapy applications. *IJN*. 2020;15:6917–6934. doi:10.2147/IJN.S264498
12. Qin Y, Wang L, Gao Z, Chen G, Zhang C. Bone marrow stromal/stem cell-derived extracellular vesicles regulate osteoblast activity and differentiation in vitro and promote bone regeneration in vivo. *Sci Rep*. 2016;6(1):21961. doi:10.1038/srep21961
13. Lu Z, Chen Y, Dunstan C, Roohani-Esfahani S, Zreiqat H. Priming adipose stem cells with tumor necrosis factor-alpha preconditioning potentiates their exosome efficacy for bone regeneration. *Tissue Engineering Part A*. 2017;23(21–22):1212–1220. doi:10.1089/ten.tea.2016.0548
14. Liu W, Yu M, Chen F, et al. A novel delivery nanobiotechnology: engineered miR-181b exosomes improved osteointegration by regulating macrophage polarization. *J Nanobiotechnol*. 2021;19(1):269. doi:10.1186/s12951-021-01015-y
15. Arabpour M, Saghazadeh A, Rezaei N. Anti-inflammatory and M2 macrophage polarization-promoting effect of mesenchymal stem cell-derived exosomes. *Int Immunopharmacol*. 2021;97:107823. doi:10.1016/j.intimp.2021.107823
16. Nakao Y, Fukuda T, Zhang Q, et al. Exosomes from TNF-α-treated human gingiva-derived MSCs enhance M2 macrophage polarization and inhibit periodontal bone loss. *Acta Biomaterialia*. 2021;122:306–324. doi:10.1016/j.actbio.2020.12.046
17. Li R, Li D, Wang H, et al. Exosomes from adipose-derived stem cells regulate M1/M2 macrophage phenotypic polarization to promote bone healing via miR-451a/MIF. *Stem Cell Res Ther*. 2022;13(1):149. doi:10.1186/s13287-022-02823-1
18. Fang P, Li X, Dai J, et al. Immune cell subset differentiation and tissue inflammation. *J Hematol Oncol*. 2018;11(1):97. doi:10.1186/s13045-018-0637-x
19. Samblas M, Martínez JA, Milagro F. Folic acid improves the inflammatory response in LPS-activated THP-1 macrophages. *Mediators Inflamm*. 2018;2018:1–8. doi:10.1155/2018/1312626
20. McDonald MK, Tian Y, Qureshi RA, et al. Functional significance of macrophage-derived exosomes in inflammation and pain. *Pain*. 2014;155 (8):1527–1539. doi:10.1016/j.pain.2014.04.029
21. Rosado MM, Simkó M, Mattsson MO, Pioli C. Immune-modulating perspectives for low frequency electromagnetic fields in innate immunity. *Front Public Health*. 2018;6:85. doi:10.3389/fpubh.2018.00085
22. Ross CL, Zhou Y, McCall CE, Soker S, Criswell TL. The use of pulsed electromagnetic field to modulate inflammation and improve tissue regeneration: a review. *Bioelectricity*. 2019;1(4):247–259. doi:10.1089/bioe.2019.0026
23. Ferroni L, Gardin C, Dolkart O, et al. Pulsed electromagnetic fields increase osteogenetic commitment of MSCs via the mTOR pathway in TNF-α mediated inflammatory conditions: an in-vitro study. *Sci Rep*. 2018;8(1):5108. doi:10.1038/s41598-018-23499-9
24. Sun W, Gan Y, Fu Y, Lu D, Chiang H. An incoherent magnetic field inhibited EGF receptor clustering and phosphorylation induced by a 50-Hz magnetic field in cultured fl cells. *Cell Physiol Biochem*. 2008;22(5–6):507–514. doi:10.1159/000185524
25. Bekhite MM, Finkensieper A, Abou–Zaid FA, et al. Static electromagnetic fields induce vasculogenesis and chondro-osteogenesis of mouse embryonic stem cells by reactive oxygen species-mediated up-regulation of vascular endothelial growth factor. *Stem Cells Dev*. 2010;19 (5):731–743. doi:10.1089/scd.2008.0266
26. Ross CL, Ang DC, Almeida-Porada G. Targeting mesenchymal stromal cells/pericytes (MSCs) with pulsed electromagnetic field (PEMF) has the potential to treat rheumatoid arthritis. *Front Immunol*. 2019;10:266. doi:10.3389/fimmu.2019.00266
27. Barak S, Matalon S, Dolkart O, Zavan B, Mortellaro C, Piattelli A. Miniaturized electromagnetic device abutment improves stability of the dental implants. *J Craniofac Surg*. 2019;30(4):1055–1057. doi:10.1097/SCS.0000000000004763
28. Zanotti F, Trentini M, Zanolla I, et al. Playing with biophysics: how a symphony of different electromagnetic fields acts to reduce the inflammation in diabetic derived cells. *IJMS*. 2023;24(2):1754. doi:10.3390/ijms24021754
29. Chachques JC, Gardin C, Lila N, et al. Elastomeric cardiowrap scaffolds functionalized with mesenchymal stem cells-derived exosomes induce a positive modulation in the inflammatory and wound healing response of mesenchymal stem cell and macrophage. *Biomedicines*. 2021;9(7):824. doi:10.3390/biomedicines9070824

30. Varani K, Padovan M, Vincenzi F, et al. A2A and A3 adenosine receptor expression in rheumatoid arthritis: upregulation, inverse correlation with disease activity score and suppression of inflammatory cytokine and metalloproteinase release. *Arthritis Res Ther*. 2011;13(6):R197. doi:10.1186/ar3527
31. Goodman R, Lin-Ye A, Geddis M, et al. Extremely low frequency electromagnetic fields activate the ERK cascade, increase hsp70 protein levels and promote regeneration in Planaria. *Int J of Radiation Biol*. 2009;85(10):851–859. doi:10.3109/09553000903072488
32. D'Amora U, Russo T, Gloria A, et al. 3D additive-manufactured nanocomposite magnetic scaffolds: effect of the application mode of a time-dependent magnetic field on hMSCs behavior. *Bioactive Materials*. 2017;2(3):138–145. doi:10.1016/j.bioactmat.2017.04.003
33. De Santis R, Gloria A, Russo T, et al. Viscoelastic properties of rapid prototyped magnetic nanocomposite scaffolds for osteochondral tissue regeneration. *Procedia CIRP*. 2016;49:76–82. doi:10.1016/j.procir.2015.07.037
34. Zhou J, Wang J, Qu M, et al. Effect of the pulsed electromagnetic field treatment in a rat model of senile osteoporosis in vivo. *Bioelectromagnetics*. 2022;43(7):438–447. doi:10.1002/bem.22423
35. Gabetti S, Masante B, Cochis A, et al. An automated 3D-printed perfusion bioreactor combinable with pulsed electromagnetic field stimulators for bone tissue investigations. *Sci Rep*. 2022;12(1):13859. doi:10.1038/s41598-022-18075-1
36. Mijiritsky E, Gardin C, Ferroni L, Lacza Z, Zavan B. Albumin-impregnated bone granules modulate the interactions between mesenchymal stem cells and monocytes under in vitro inflammatory conditions. *Mater Sci Eng*. 2020;110:110678. doi:10.1016/j.msec.2020.110678
37. Gardin C, Bosco G, Ferroni L, et al. Hyperbaric oxygen therapy improves the osteogenic and vasculogenic properties of mesenchymal stem cells in the presence of inflammation in vitro. *IJMS*. 2020;21(4):1452. doi:10.3390/ijms21041452
38. Trentini M, Zanolla I, Zanotti F, et al. Apple derived exosomes improve collagen type i production and decrease MMPs during aging of the skin through downregulation of the NF-κB pathway as mode of action. *Cells*. 2022;11(24):3950. doi:10.3390/cells11243950
39. Brunello G, Zanotti F, Trentini M, et al. Exosomes derived from dental pulp stem cells show different angiogenic and osteogenic properties in relation to the age of the donor. *Pharmaceutics*. 2022;14(5):908. doi:10.3390/pharmaceutics14050908
40. Gardin C, Ferroni L, Erdoğan YK, et al. Nanostructured modifications of titanium surfaces improve vascular regenerative properties of exosomes derived from mesenchymal stem cells: preliminary in vitro results. *Nanomaterials*. 2021;11(12):3452. doi:10.3390/nano11123452
41. Zanotti F, Zanolla I, Trentini M, et al. Mitochondrial metabolism and ev cargo of endothelial cells is affected in presence of evs derived from MSCs on which hif is activated. *IJMS*. 2023;24(6):6002. doi:10.3390/ijms24066002
42. Ramzan F, Salim A, Khan I. Osteochondral tissue engineering dilemma: scaffolding trends in regenerative medicine. *Stem Cell Rev and Rep*. 2023;19(6):1615–1634. doi:doi:10.1007/s12015-023-10545-x
43. Dong C, Tan G, Zhang G, Lin W, Wang G. The function of immunomodulation and biomaterials for scaffold in the process of bone defect repair: a review. *Front Bioeng Biotechnol*. 2023;11:1133995. doi:10.3389/fbioe.2023.1133995
44. Zhou J, Xiong S, Liu M, et al. Study on the influence of scaffold morphology and structure on osteogenic performance. *Front Bioeng Biotechnol*. 2023;11:1127162. doi:10.3389/fbioe.2023.1127162
45. Zhang J, Xu H, Han Z, et al. Pulsed electromagnetic field inhibits RANKL-dependent osteoclastic differentiation in RAW264.7 cells through the Ca 2+ -calcineurin-NFATc1 signaling pathway. *Biochem Biophys Res Commun*. 2017;482(2):289–295. doi:10.1016/j.bbrc.2016.11.056
46. Chen Y, Menger MM, Braun BJ, et al. Modulation of macrophage activity by pulsed electromagnetic fields in the context of fracture healing. *Bioengineering*. 2021;8(11):167. doi:10.3390/bioengineering8110167
47. Song X, Xue Y, Fan S, Hao J, Deng R. Lipopolysaccharide-activated macrophages regulate the osteogenic differentiation of bone marrow mesenchymal stem cells through exosomes. *PeerJ*. 2022;10(e13442):e13442. doi:10.7717/peerj.13442
48. Zhou Y, Hu G. M2 macrophages-derived exosomes regulate osteoclast differentiation by the CSF2/TNF-α axis. *BMC Oral Health*. 2024;24(1):107. doi:10.1186/s12903-023-03842-x
49. Chen X, Wan Z, Yang L, et al. Exosomes derived from reparative M2-like macrophages prevent bone loss in murine periodontitis models via IL-10 mRNA. *J Nanobiotechnol*. 2022;20(1):110. doi:10.1186/s12951-022-01314-y
50. Bressan E, Ferroni L, Gardin C, et al. Metal nanoparticles released from dental implant surfaces: potential contribution to chronic inflammation and peri-implant bone loss. *Materials*. 2019;12(12):2036. doi:10.3390/ma12122036
51. Ramos Xavier Coutinho Nascimento L, Monteiro Torelly G, Nelson Elias C. Analysis of bone stress and primary stability of a dental implant using strain and torque measurements. *Saudi Dent J*. 2023;35(3):263–269. doi:10.1016/j.sdentj.2023.01.006
52. Nayak BP, Dolkart O, Satwalekar P, et al. Effect of the pulsed electromagnetic field (PEMF) on dental implants stability: a randomized controlled Clinical trial. *Materials*. 2020;13(7):1667. doi:10.3390/ma13071667
53. Schermann H, Gurel R, Gold A, et al. Safety of urgent hip fracture surgery protocol under influence of direct oral anticoagulation medications. *Injury*. 2019;50(2):398–402. doi:10.1016/j.injury.2018.10.033